Journal of Virological Methods 329 (2024) 114993

Contents lists available at ScienceDirect

Journal of Virological Methods

journal homepage: www.elsevier.com/locate/jviromet

Protocols

A novel digital PCR assay for detection and comprehensive characterization of *Molluscum contagiosum virus* genotypes MOCV1, MOCV2, and MOCV3 and recombinant lineages

Tomaž M. Zorec [a,b,1], Lucijan Skubic [a,1], Mario Poljak [a,*]

[a] *Institute of Microbiology and Immunology, University of Ljubljana, Zaloška 4, Ljubljana, Slovenia*
[b] *Celica Biomedical, Tehnološki park 24, Ljubljana, Slovenia*

ARTICLE INFO

Keywords:
Molluscum contagiosum
Molluscum contagiosum virus
Digital PCR
Molecular diagnostics
Diversity screening
Sample prioritization triage

ABSTRACT

Molluscum contagiosum virus (MOCV) is an important human pathogen causing a high disease burden worldwide. It is the last exclusively human-infecting poxvirus still circulating in its natural reservoir—a valuable model of poxviral evolution. Unfortunately, MOCV remains neglected, and little is known about its evolutionary history and circulating genomic variants, especially in non-privileged countries. The design weaknesses of available MOCV detection/genotyping assays surfaced with recent accumulation of abundant sequence information: all existing MOCV assays fail at accurate genotyping and capturing sub-genotype level diversity. Because complete MOCV genome characterization is an expensive and labor-intensive task, it makes sense to prioritize samples for whole-genome sequencing by diversity triage screening. To meet this demand, we developed a novel assay for accurate MOCV detection and genotyping, and comprehensive sub-genotype qualification to the level of phylogenetic groups (PGs). The assay included a novel set of oligonucleotide primers and probes, and it was implemented using digital polymerase chain reaction (dPCR). It offers sensitive, specific, and accurate detection, genotyping (MOCV1–MOCV3), and PG qualification (PG1–6) of MOCV DNA from clinical samples. The novel dPCR assay is suitable for MOCV diversity triage screening and prioritization of samples for complete MOCV genome characterization.

1. Introduction

Molluscum contagiosum virus (MOCV), the causative agent of molluscum contagiosum (MC), is the last still naturally circulating exclusively human-infecting poxvirus since the eradication of smallpox. Until the characterization of the equine molluscum contagiosum–like virus, MOCV was the only member of the unique taxonomic genus *Molluscipoxvirus* (Chen et al., 2013; Ehmann et al., 2021). MC is one of the 50 most prevalent diseases of humans and has a high disease burden (Konya and Thompson, 1999; Hay et al., 2014; Sherwani et al., 2014). In addition, MC is a very opportune model for observing the evolution of an exclusively homo-tropic poxvirus in its natural circulation.

Four MOCV genotypes (MOCV1–4) and three subtype variants of MOCV1 (MOCV1va, MOCV1vb, and MOCV1vc) were identified with complete genome restriction profiling in early molecular epidemiological studies of MOCV (Blake et al., 1991; Nakamura et al., 1995). Partial genome sequences of MOCV1 and MOCV2, which primarily included parts of the MOCV gene MC021L, have been known since the early 1990s (Porter and Archard, 1992). The first complete genome sequences of MOCV1, MOCV2, and MOCV3 became available later, in 1996 (Senkevich et al., 1996), 2017 (López-Bueno et al., 2017), and 2023 (Zorec et al., 2023), respectively. Recombination analysis revealed the presence of three genomic regions in the MOCV genomes that are inter-genotype recombination hot-spots (RS1, RS2, and RS3) (López-Bueno et al., 2017; Zorec et al., 2018). Recently, sequence-based analysis of restriction patterns in 66 complete MOCV genomes suggested that the MOCV subtype variants MOCV1va and MOCV1vc from the early studies emerged through recombination at RS1 and RS2; phylogenetically, the legacy MOCV subtype variants formed six distinct phylogroups (PGs): PG1—PG6 (Zorec et al., 2023).

Cross-reference with historical data shows that genomic sequences of MOCV4 and the subtype variant MOCV1vb have not yet been recorded,

* Corresponding author.
E-mail address: mario.poljak@mf.uni-lj.si (M. Poljak).
[1] These authors contributed equally

https://doi.org/10.1016/j.jviromet.2024.114993
Received 23 April 2024; Received in revised form 26 June 2024; Accepted 27 June 2024
Available online 1 July 2024

and there may be other MOCV genotypes and molecular variants still undetected (Zorec et al., 2023). MOCV molecular variants are spread unevenly, and their prevalence ratios vary regionally, with reliable information on MOCV diversity limited to a handful of countries: Australia, Germany, Iran, Japan, Turkey, Slovenia, Spain, the United Kingdom, and the United States (Konya and Thompson, 1999; Porter and Archard, 1992; Nakamura et al., 1995; Nuñez et al., 1996; Yamashita et al., 1996; Thompson, 1997; Agromayor et al., 2002; Saral et al., 2006; Sherwani et al., 2014; Trčko et al., 2016, 2018; Taghinezhad-S et al., 2018). Because MOCV have complicated genomes approximately 190 kb long with around 182 genes, repetitive regions, and inverted terminal repeats (Senkevich et al., 1996, 1997), it may not be feasible to characterize the complete MOCV genome sequences from each individual clinical sample. Instead, a comprehensive triage strategy to select the most appropriate samples for complete viral genome sequencing would be useful.

Available MOCV detection and genotyping assays have so far been limited to MOCV1 and MOCV2. They have been based on Southern blotting (Konya and Thompson, 1999), polymerase chain reaction (PCR) amplification of specific MOCV genomic regions followed by restriction endonuclease cleavage (Nuñez et al., 1996) or amplicon sequencing (Thompson, 1997; Trama et al., 2007) or quantitative genotype-specific real time PCR (qPCR) (Hošnjak et al., 2013). Recently generated abundant sequence data (Zorec et al., 2023) show that the currently available PCR-based assays (Nuñez et al., 1996; Hošnjak et al., 2013) fail to accurately qualify the known MOCV genotypes. Although amplicon sequencing of the genome fragment targeted in the assay by Hošnjak et al. (2013), as suggested by Trama et al. (2007), may provide accurate resolution of the MOCV1, MOCV2, and MOCV3 genotypes, it does not provide PG qualification or any other indication of genomic diversity.

qPCR is an established digital PCR (dPCR) that is a promising molecular diagnostic platform allowing MOCV detection and quantification as well as characterization of MOCV genotypes and their sub-genotype diversity: PGs. With equivalent oligonucleotide primer and probe systems, superior reproducibility, resilience to PCR inhibitors, and direct absolute quantification of target DNA are the main advantages of dPCR over qPCR (Quan et al., 2018).

Here, we describe a novel dPCR-based assay for comprehensive detection, absolute quantification, and characterization of MOCV down to the genotype level (MOCV1–MOCV3), as well as the known PGs (PG1–6). To the best of our knowledge, this is the first dPCR-based assay for MOCV. We designed a novel panel of eight sets of specific oligonucleotide primers and hydrolysis probes, which targeted seven different genomic regions distributed across MOCV genomes and are used in multiplexed PCR reactions. We show that the novel dPCR-based assay is specific, sensitive, qualitatively and quantitatively accurate, and suitable for MOCV diversity triage screening and prioritization of samples for complete MOCV genome characterization.

2. Materials and methods

2.1. Primers and probes

We developed a panel of eight sets of oligonucleotide primers and fluorescently labeled hydrolysis probes (Table 1) to detect, quantify, and comprehensively characterize MOCVs in clinical samples to the levels of genotypes and PGs. PGs were determined by testing sequence states at the recombinant segments *RS1* and *RS2*. It was previously shown that PGs can be inferred from the combination of genotype and sequence states E0, E1, or E2 at *RS1* and E0 or E1 at *RS2* (Zorec et al., 2023); this feature is exploited here (Table 2). The oligo panel was designed based on a multiple sequence alignment (MSA) of 66 complete MOCV genomes downloaded from the GenBank database (NCBI, 2023) (see **Appendix B** for details). The alignments of the oligo sets with the MSA are shown in

Table 1
Oligonucleotide primers and hydrolysis probes for detection, quantification, and qualification of MOCV genotypes (MOCV1-3) and recombination states at *RS1* (E0, E1, and E2) and *RS2* (E0 and E1).

Diagnostic concept	Set no.	Sequence name	Sequence (5′ → 3′)	Target sequence coordinates (a = amplicon, p = probe)
Detection and quantification	1	MOCV-Forward	CAAGGCGAAATGAAAACATCAG	a U60315.168682—168861
		MOCV-Reverse	ATCGGATGCAAAGACGGTACA	
		MOCV-Probe	FAM-TCAGGGTTTTGGTTTTGTGGACAGG-BHQ1	p U60315.168760—168784
Genotyping	2	MOCV1-Forward	CTGGAGTTCGAGAAGCAGGAA	a U60315.151408—151576
		MOCV1-Reverse	GCGGAAAGACACGGTCTCAT	
		MOCV1-Probe	HEX-TGGGCTAGGAGGGGAAAGATGAAGC-BHQ1	p U60315.151478—151502
	3	MOCV2-Forward	GAGTACGCAGGCGAGACTTTC	a KY040274.49791—49943
		MOCV2-Reverse	GCGGAAAGACACGGTCTCAT	
		MOCV2-Probe	Cy5-CTTGTTCCAGAAGAAGCTGTCGGGC-BHQ2	p KY040274.49884—49908
	4	MOCV3-Forward	TTCAACAACACGCACGAGTCT	a OQ401160.177208—177376
		MOCV3-Reverse	TACACATGCCTTCAGGAACGA	
		MOCV3-Probe	TAMRA-CAGCACCACCAGCAGAGCCATTG-BHQ2	p OQ401160.177272—177294
Determination of recombination status	5	RS1E0-Forward	AGACGGCGTTGGTGACTACG	a U60315.43944—44102
		RS1E0-Reverse	AGAGGGCGGTCTCCTAGCTG	
		RS1E0-Probe	FAM-CAGGACGCAGACGAGGACATGGTC-BHQ1	p U60315.43994—44017
	6	RS1E1-Forward	AGAGTACGCACGCAGGCAC	a KY040276.41805—42025
		RS1E1-Reverse	CGAAGTGAATCTCCGAGTGCT	
		RS1E1-Probe	Cy5-CTCCCAGGGTACGCAGACTGTCACG-BHQ2	p KY040276.41920—41944
	7	RS1E2-Forward	GAGAAGACACTCGCAAGTACGG	a MH320556.41731—41906
		RS1E2-Reverse	GGAGCCATCTTGAGCGTACTC	
		RS1E2-Probe	TAMRA-TGGAACACACACTGTCACATGGACTCCTT-BHQ2	p MH320556.41808—41836
	8	RS2-Forward	TCTTGGKTTKCCACCGAGA	a U60315.74419—74539
		RS2-Reverse	GGAACTTGACAAGATGGRSTCT	
		RS2E0-Probe	HEX-TTGGGTGTGAAGCCACTTGTCAACG-BHQ1	p U60315.74472—74496
		RS2E1-Probe	ROX-ATGCGAGACACGGGACGCTTGTT-BHQ2	p KY040276.74088—74110

Table 2
Phylogroup (PG) is determined by the combination of MOCV genotype and recombination state at *RS1* and *RS2*.

Phylogroup	MOCV genotype	*RS1*	*RS2*
PG1	MOCV1	E0	E0
PG2	MOCV1	E0	E1
PG3	MOCV1	E1	E1
PG4	MOCV2	E1	E0
PG5	MOCV2	E2	E0
PG6	MOCV3	E1	E0

Appendix A: Supplementary Figures **A.2.1-A.2.7**.

The MSA was prepared using Mafft v7.407 software (Katoh and Standley, 2013). Candidate oligo sets were generated using the web application Primer3 v0.4.0 (Koressaar and Remm, 2007; Untergasser et al., 2012). Evaluation and downstream selection of oligo sets was facilitated by inspecting annealing energetics as predicted by the web application Net Primer (PREMIER Biosoft, 2023). Finally, web-based NCBI Nucleotide BLAST searches were performed versus the NT database to ensure oligo specificity (NCBI, 2023).

The oligonucleotide primers were synthesized and supplied by Integrated DNA Technologies (Integrated DNA Technologies BVBA—IDT, Leuven, Belgium). Fluorescently labeled hydrolysis probes were synthesized and supplied by TIB Molbiol (TIB Molbiol, Berlin, Germany).

2.2. Control, verification, and test samples

The oligo panel was verified and tested using 23 MOCV-positive DNA isolates from clinically visible MC lesions collected by curettage procedure (samples 1–7 and 11–26; Table 3) in our previous studies (Hošnjak et al., 2013; Trčko et al., 2016, 2018; Zorec et al., 2018, 2023). Total DNA was extracted using QIAmp DNA Mini Kit (Qiagen, Hilden, Germany) and stored at −20 °C.

Samples 1–7 were used for primary assay verification. The MOCV genome sequences in these samples were characterized to the complete genome level during previous studies (Zorec et al., 2018, 2023). These seven samples represented the genotypes MOCV1 and MOCV2, and PG1, PG2, PG4, and PG5.

No samples representing MOCV1—PG3 and MOCV3—PG6 are available in our archives. However, PG3 corresponds to MOCV1 with the recombinant sequence states *RS1E1* and *RS2E1* **(**Table 2**)**, and these are already covered in samples 3 and 4 (PG4), and in sample 2 (PG2), respectively.

Positive validation controls for MOCV3 (PG6) were synthetic double-stranded DNA fragments that encapsulated the panels' amplicon sequences used for (i) MOCV detection/quantification—sample 8 (OQ401160.168252–168430; gBlocks, IDT), (ii) identification of MOCV3—sample 9 (OQ401160.177193–177391; Ultramer DNA Oligos, IDT), and (iii) the amplicon sequence of MOCV3 targeted with the oligo set for sensing the sequence state at *RS2*—sample 10 (OQ401160.74487–74790; gBlocks, IDT). All synthetic double-stranded DNA fragments were resuspended in nuclease-free water (Qiagen) prior to use, as instructed by the manufacturer. For sequence details on the synthetic DNA fragments, see **Appendix A: A.1** Supplementary Data.

The test set included 16 clinical samples (samples 11–26), which were partially characterized during previous studies at various subgenomic levels using qPCR and described in Hošnjak et al. (2013), and partial gene sequences of *MC021L*, *MC097R*, and *MC148R*. These samples were selected to maximize phylogenetic diversity to the best of our knowledge.

Two whole DNA isolates of monkeypox virus (mpox; samples 27 and 28) collected and isolated during the 2022 outbreak in Slovenia (Resman Rus et al., 2023) were used as negative controls to demonstrate the absence of oligo cross-reactivity with mpox and orthopoxviruses. MOCV-free human genomic DNA (sample 29; Roche Diagnostics, Mannheim, Germany) was used as a negative control to demonstrate the absence of oligo cross-reactivity with human DNA. Nuclease-free water with no DNA template was used in all PCR runs as a reference control for potential amplicon carryover contamination (sample 30).

The table includes previously determined MOCV genotype and PG information, level of prior evidence, and results of testing using the novel dPCR assay. The test outcomes for each target tested are indicated with a plus or minus. Multiple pluses or minuses in the result field indicate test replication. Dashed borders delimit samples with comprehensive MOCV and PG prior information, samples with incomplete genotype/PG information, and negative control samples. Two samples tested positive to multiple (two) molecular species; genotyping and PG-qualification results are marked with an asterisk. CGC = complete genome characterization; qPCR = results of qPCR by Hošnjak et al. (2013); DESIGN = synthetic double-stranded DNA fragments; MC021L/MC079R/MC148R = partial coding sequence sequencing.

2.3. Assay implementation

2.3.1. Digital PCR

The assay was implemented using the QIAcuity nanoplate-based microfluidic dPCR platform (Qiagen) in three multiplex/singleplex reactions: (i) a multiplex dPCR (oligo sets 1–4; Table 1) for MOCV detection, quantification, and genotyping, (ii) a multiplex dPCR (oligo sets 5, 6, and 8) for detecting recombination states at *RS1* and *RS2*, and (iii) a singleplex dPCR (oligo set 7) for detection of *RS1* E2.

dPCRs were performed using the QIAcuity Probe PCR Kit (Qiagen) in 40 µl reaction mixtures, each containing 10 µl of sample DNA, 10 µl of 4x Probe PCR Master Mix, 0.4 µM of each of the specific primers and 0.2 µM of each of the specific probes, 0.025 IU/µl of the restriction enzyme Anza 52 *Pvu*II (Thermo Scientific, Waltham, MA, USA), and nuclease-free water. The reaction mixtures were prepared in pre-plates, transferred to the QIAcuity Nanoplate 26k 24-well plate (Qiagen), sealed with the QIAcuity Nanoplate Seal (Qiagen), and loaded onto the automated dPCR instrument QIAcuity Four (Qiagen), as instructed by the manufacturer. The workflow included: (i) a priming and rolling step with well partitioning; (ii) a thermocycling step including initial DNA denaturation and enzyme activation at 95 °C for 2 min, 45 amplification cycles of 15 s at 95 °C, and 1 min at 60 °C; and (iii) an imaging step with image acquisition. Depending on dye excitation/fluorescence spectra of the target specific hydrolysis probes, image acquisition settings at the relevant color channels were green channel (excitation exposure time 500 ms, gain 6 dB), yellow channel (excitation exposure time 500 ms, gain 6 dB), orange channel (excitation exposure time 400 ms, gain 6 dB), red channel (exposure time 300 ms, gain 4 dB), and crimson channel (excitation exposure time 400 ms, gain 8 dB).

RS1 E2 was detected using the singleplex dPCR. To optimize the *RS1* E2 dPCR, the oligo set 7 was tested at an annealing temperature of 60 °C with different primer-probe concentrations in the reaction mixture (see **Appendix A:** Supplementary Figure **A.2.8 A**). The optimal *RS1* E2 dPCR reaction mixture contained 0.9 µM of each of the specific primers and 0.4 µM of the specific probe. Different image acquisition settings were also tested to optimize fluorescence signal resolution between negative and positive control samples. We varied exposure times between 400 and 800 (step 100 ms) and signal gains between 4 and 10 dB (step 1 dB). Finally, the fluorescence signal was measured at the orange channel with an exposure time of 800 ms and gain of 10 dB.

Sample 9, used as positive validation control for qualification of MOCV3, initially showed a wide distribution with slight negative skew in above-baseline partition intensity in the multiplex dPCR. Because the positive signal scatter partially overlapped with baseline, we attempted to optimize the parameters for this dPCR. We tested sample 9 in singleplex dPCRs with different primer-probe concentrations (oligo set 4) in the reaction mixtures and at annealing temperatures of 56 °C (see **Appendix A:** Supplementary Figure **A.2.8B**) and 62 °C (see **Appendix A:** Supplementary Figure **A.2.8 C**), respectively. However, the varied parameters had no notable effect on reducing scatter and negative skew

Table 3
Sample metadata, prior information, and test results.

Sample no.	GenBank acc. no. / standard name	Genotype (prior)	PG (prior)	RS1 (prior)	RS2 (prior)	Prior tests / knowledge	dPCR test result										
							Detection	Genotype			Recombination status					Genotype	PG
											RS1			RS2			
								1	2	3	E0	E1	E2	E0	E1		
1	MN931744	MOCV1	PG1	E0	E0	CGC	++	++	−−	−−	++	−−	−−	++	−−	MOCV1	PG1
2	MH320547	MOCV1	PG2	E0	E1	CGC	++	++	−−	−−	++	−−	−−	−−	++	MOCV1	PG2
3	MN931751	MOCV2	PG4	E1	E0	CGC	++	−−	++	−−	−−	++	−−	++	−−	MOCV2	PG4
4	MH320549	MOCV2	PG4	E1	E0	CGC	++	−−	++	−−	−−	++	−−	++	−−	MOCV2	PG4
5	MH320548	MOCV2	PG4	E1	E0	CGC	++	−−	++	−−	−−	++	−−	++	−−	MOCV2	PG4
6	MN931750	MOCV2	PG5	E2	E0	CGC	++	−−	++	−−	−−	−−	++	++	−−	MOCV2	PG5
7	MN931752	MOCV2	PG5	E2	E0	CGC	++	−−	++	−−	−−	−−	++	++	−−	MOCV2	PG5
8	(OQ401160)	(MOCV3)	(PG6)	/ (E1)	/ (E0)	DESIGN	++	−−	−−	−−	−−	−−	−−	−−	−−		
9	(OQ401160)	MOCV3	(PG6)	/ (E1)	/ (E0)	DESIGN	−	−	−	+	−	−	−	−	−	MOCV3	PG6
10	(OQ401160)	(MOCV3)	(PG6)	/ (E1)	E0	DESIGN	−−	−−	−−	−−	−−	−−	−−	++	−−		
11		MOCV1				qPCR, MC148R	++	++	−−	−−	++	−−	−−	−−	++	MOCV1	PG2
12		MOCV1				qPCR, MC021L, MC148R	++	++	−−	−−	++	−−	−−	++	−−	MOCV1	PG1
13		MOCV2				qPCR, MC079R	++	++	++	−−	++	++	−−	++	++	MOCV1+MOCV2 *	PG2+ PG4 *
14		MOCV2				qPCR, MC079R, MC148R	++	−−	++	−−	−−	++	−−	++	−−	MOCV2	PG4
15		MOCV1				qPCR, MC079R	++	++	−−	−−	++	−−	−−	−−	++	MOCV1	PG2
16		MOCV1				qPCR, MC079R	++	++	−−	−−	++	−−	−−	−−	++	MOCV1	PG2
17		MOCV1				qPCR, MC079R	++	++	−−	−−	++	−−	−−	−−	++	MOCV1	PG2
18		MOCV1				qPCR, MC079R	++	++	++	−−	++	++	−−	++	−−	MOCV1+MOCV2 *	PG1+ PG4 *
19		MOCV1				qPCR, MC079R, MC148R	++	++	−−	−−	++	−−	−−	++	−−	MOCV1	PG2
20		MOCV2				qPCR, MC021L, MC079R, MC148R	++	−−	++	−−	−−	−−	++	++	−−	MOCV2	PG5
21		MOCV2				qPCR, MC021L, MC079R, MC148R	++	−−	++	−−	−−	−−	++	++	−−	MOCV2	PG5
22		MOCV1				qPCR, MC148R	++	++	−−	−−	++	−−	−−	++	−−	MOCV1	PG1
23		MOCV1				qPCR, MC079R, MC148R	++	++	−−	−−	++	−−	−−	−−	++	MOCV1	PG5
24		MOCV1				qPCR, MC079R, MC148R	++++	++++	−−−−	−−−−	++++	−−−−	−−−−	−−−−	++++	MOCV1	PG5
25		MOCV1				qPCR, MC148R	+	−	+	−	−	+	−	+	−	MOCV2	PG4
26		MOCV2				qPCR, MC079R, MC148R	++	−−	++	−−	−−	−−	++	++	−−	MOCV2	PG5
27						Mpox Isolated on Vero cells	−	−	−	−	−	−	−	−	−		
28						Mpox Isolated on Vero cells	−	−	−	−	−	−	−	−	−		
29						HUMAN NON-MOCV	−	−	−	−	−	−	−	−	−		
30						Water	−−−−	−−−−	−−−−	−−−−	−−−−	−−−−	−−−−	−−−−	−−−−		

in signal intensity distribution in this case.

To improve the accuracy of the concentration calculation in each well, Volume Precision Factor v6.0 (Qiagen) was applied according to the manufacturer's instructions. Raw dPCR data were analyzed using QIAcuity Software Suite v2.5.0.1 (Qiagen). Fluorescence intensity thresholds were set at the highest intensity values recorded in non-template blank experiments.

The presence and concentration of MOCV were evaluated using the fluorescence signal of oligo set 1 at the green channel. The other channels were used for detection of the specific MOCV genotypes: yellow—MOCV1 (oligo set 2), crimson—MOCV2 (oligo set 3), and orange—MOCV3 (oligo set 4). Recombination states targeted by oligo sets 5–8 were read at the green (*RS1* E0), crimson (*RS1* E1), orange (*RS1* E2), yellow (*RS2* E0), and red (*RS2* E1) channels.

dPCR is sensitive to positive fluorescence signal saturation, which can result in underestimation of sample template DNA concentration (Falzone et al., 2020). Due to the excessively high concentration of MOCV DNA, the MOCV-positive samples were tested in two consecutive 10-fold dilutions, the measurements of which were subsequently used to determine the concentration of MOCV DNA in the original samples (**Appendix C**). All 10-fold serial dilutions were prepared manually in 1.5 ml DNA LoBind tubes (Eppendorf, Hamburg, Germany) using a water solution with carrier RNA (1 μg/ml) (Qiagen).

Quantitative accuracy and operative range of the assay for MOCV DNA concentration measurement were verified by testing triplicates of 10-fold serially diluted sample 8, corresponding to the input concentration range of 1×10^{6} to 1×10^{-1} copies (cp) of target DNA per reaction. The dilution series were tested both in multiplex dPCR containing oligo sets 1–4 as in multiplex dPCR for MOCV detection, quantification, and genotyping (see above) and in singleplex dPCR containing only oligo set 1. Lower bound of the assays operative range were determined by fitting target detection (endogenous dichotomous variable) to the concentrations of the standard dilution series (exogenous continuous variable) using probit models (using python statsmodels module v0.14.0). Lower bound threshold counts of positive partitions for valid readings were set based on probit model results. Relative deviation from expected concentration (RD = |Measured concentration – Expected concentration| / Expected concentration) was evaluated for each datum. Final lower and upper bounds of the assays range of accuracy was evaluated by probit fitting expected concentrations to RD<0.2 as endogenous dichotomous variable in a probit regression model. Minimum reported counts of positive and negative partitions at lower and upper bounds were also used as cutoffs for reading validity in the MOCV detection/quantification dPCR, which were set at 4 and 9 partitions respectively. An additional positive partition count threshold was set at 10 for determining MOCV genotype and recombination state qualification results. This threshold minimized false positive readings which could be recognized by reviewing the assays reported sample concentrations. Samples were tested in two consecutive 10-fold dilutions and sample concentrations were effectively recalculated to original sample dilution knowing the dilution factors (**Appendix C**). While equivalent sample concentrations would be recalculated from correct results, reported sample concentrations of these artifacts resulted in very diverging estimations.

Overloading analysis was used to evaluate primer-probe cross-target specificity at high template concentrations (**Appendix A:** Supplementary Figures **A.2.9–11**). Samples 1, 2, 3, 6, 9, 13 and 30, and 1, 2, 3, 6, 7, 10, 13 and 30 were used in the scopes of MOCV detection/genotype qualification, and recombination state qualification dPCRs, respectively. The original samples were diluted to concentrations around the assay's upper operational limits and evaluated using the multiplex dPCR assay.

2.3.2. Real-time quantitative PCR screen

A multiplex qPCR screen was implemented to find optimal dilution ranges for accurate sample quantification through qPCR quantification cycle (Cq) values. The qPCR screen was performed using the LightCycler 480 Probes Master kit (Roche Diagnostics) in a 20 μl reaction mixture, consisting of 5 μl of sample DNA, 10 μl 2× LightCycler 480 Probes Master, 0.4 μM of each of the specific primers, 0.2 μM of each of the specific probes (oligo sets 1–4; Table 1), and nuclease-free water. The qPCR amplifications were performed using a QuantStudio 7 Pro instrument (Applied Biosystems, Life Technologies, Carlsbad, CA, USA) under the following conditions: initial DNA denaturation for 10 min at 95 °C (temperature transition rate of 1.6 °C/s), followed by 45 amplification cycles of 10 s at 95 °C (1.6 °C/s), 30 s at 60 °C (1.6 °C/s), and 1 s at 72 °C (1.6 °C/s). Acquisition of the fluorescence signal was performed on specific fluorescence detection channels in a single mode at the end of the elongation step of each amplification cycle. The last step consisted of cooling the reaction mixture to 40 °C with a 30 s hold (1.6 °C/s). The qPCR results were analyzed using Design & Analysis Software v2.6.0 (Applied Biosystems).

3. Results

3.1. Specific detection of MOCV

The novel dPCR-based assay specifically detected MOCV only. All available MOCV-positive clinical samples, including PG1–2 and PG4–5, and the samples with synthetic double-stranded DNA fragments covering MOCV3, tested positive (Table 3). On the other hand, all negative controls, including nuclease-free water, MOCV-free human genomic DNA sample, and whole DNA isolates with mpox virus tested negative. The outcomes of all replicated tests were consistent with each other. Exemplar dPCR scatter plots depicting dPCR partition fluorescence intensities at the color channels reporting individual molecular targets relevant to MOCV detection and quantification, and qualification of MOCV genotypes and PGs, are shown in **Appendix A:** Supplementary Figures **A.2.12–A.2.15**. Comprehensive details on the results of each test are available in **Appendix C**.

3.2. Sensitive detection and accurate quantification of MOCV DNA

We evaluated the analytical detection limits and the quantitative accuracy of the dPCR assay for MOCV detection, quantification, and genotyping. Triplicated 10-fold serial dilutions of MOCV DNA in sample 8, the synthetic double stranded DNA fragment, were tested in multiplex and singleplex dPCR, using oligo sets 1–4 and 1, respectively. We could detect MOCV DNA at concentrations as low as 1 cp/μl reaction in 1/6 replicates, but the assay reported consistent and quantitatively accurate (RD < 0.2) readings only between 10 cp/μl and 10^{5} cp/μl (Table 4, Fig. 1, **Appendix D).** The coefficients of variation at the bounds of the assay's operational concentration range were 12 % and 4 %.

Descriptive statistics were estimated from six replicated measurements. A discrepancy from the linear relationship between the expected and measured analyte concentration was observed in elevated Σ RD below dilution level 10 cp/μl. *SD* = standard deviation, CV = coefficient of variation, Σ RD = summed relative deviation from expected concentration ($\Sigma_{\text{dilution level}}$ [(Measured concentration − Expected

Table 4
MOCV DNA quantification validation summary.

Expected concentration [cp/μl]	Measured concentration			
	Mean [cp/μl]	*SD* [cp/μl]	CV	Σ RD
0.00	0.00	0.00	—	0.00
0.10	0.00	0.00	—	6.00
1.00	0.37	0.90	2.45	6.20
10.00	10.18	1.22	0.12	0.66
100.00	102.75	9.40	0.09	0.48
1000.00	1014.87	96.10	0.09	0.48
10,000.00	9906.00	467.45	0.05	0.24
100,000.00	105,396.00	4606.65	0.04	0.36
1000,000.00	325,932.67	255,196.44	0.78	4.04

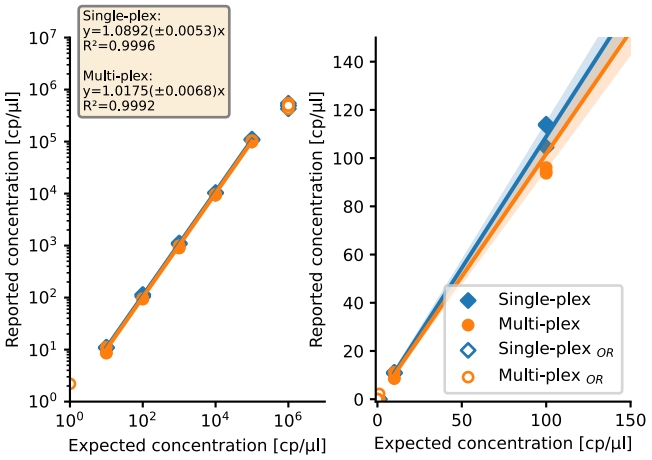

Fig. 1. MOCV DNA quantification—validation curve. MOCV DNA concentration reported by the dPCR assay is plotted versus expected concentrations of non-template control samples (water) and a 10-fold serial dilution series of sample 8 (10^{-1} - 10^{6} cp/µl). Results are shown for single and multiplex dPCR. Each datum is shown in triplicate. Data are plotted in logarithmic scale **(left)** between standard concentrations 10^{0} and 10^{6} cp/µl and in linear scale between 0 and 150 cp/µl (**right**). Deviations from linearity appeared at concentrations below 10 cp/µl and above 10^{5} cp/µl. These points were out of the assays' operative concentration range (OR). Data within OR are shown with filled plot markers and were included in linear regression. CI99 of the regression predictions are illustrated with shading. Data outside OR (denoted as OR) are shown with empty plot markers. The MOCV DNA concentration measured by the dPCR assay was in a linear relationship with the expected concentration ($R^2_{singleplex}$ = 0.9992, $R^2_{multiplex}$ = 0.9996). Singleplex and multiplex dPCR experiments were consistent with each other.

concentration) / Expected concentration]).

3.3. Accurate qualification of MOCV genotypes and phylogroups

The novel dPCR-based assay was successfully applied to MOCV genotyping and PG qualification. The assay correctly qualified the MOCV genotype in all tested DNA isolates from clinical samples (samples 1–7 and 11–26), including MOCV1 and MOCV2, and PG1–2 and PG4–5 (Table 3). All relevant samples tested consistently with *a priori* PG information (samples 1–7). Assay validity for MOCV3 (PG6) was comprehensively tested using synthetic double-stranded DNA fragments encapsulating MOCV3 sequence probe annealing locations (samples 8–10; see **2.2. Control, verification, and test samples** for details)—all three synthetic DNA fragments tested consistently with sequence design. The assay correctly identified all features characteristic for PG3 (MOCV1, E1 at *RS1*, and E1 at *RS1*) and thus confirmed that PG3 can also be detected and characterized using the novel assay.

Finally, samples 11–26 were characterized to the level of PGs for the first time (See **Appendix C** for complete results). Among these 16 samples, the novel assay found PG1 in two samples, PG2 in five samples, PG4 in two samples, and PG5 in five samples (Table 3). We found no new samples with PG3 or PG6 (MOCV3).

Overloading analysis showed no off-target reactivity of oligo sets at high template concentrations, up to the assay's upper operational concentration limit, 10^{5} cp/µl. Beyond this point, we noted off-target reactivity with oligo sets 4 (MOCV3) and 8 (RS2E1), and samples of MOCV1 and MOCV2 PG5, respectively (**Appendix A:** Supplementary Figures **A.2.9–11**).

3.4. Simultaneous detection of multiple MOCV genotypes in individual samples

The novel dPCR-based assay suggested the presence of at least two different molecular species, the genotypes MOCV1 and MOCV2, in samples 13 and 18 (Table 3). The combination of genotype and recombination states suggested the presence of PG2 and PG4 in sample 13, and PG1 and PG4 in sample 18. We consulted the results for these samples from prior experiments using the qPCR protocol (Hošnjak et al. 2013): sample 13 previously tested as MOCV2 and sample 18 as MOCV1. However, the partial gene sequence from sample 13 positioned alongside MOCV1 and not MOCV2. In addition to an MOCV1 hallmark peak at 60–62 °C in dF/dT (dF = ratio between fluorescence intensities at 640 nm and 530 nm), used for genotype qualification therein, sample 18 also showed an abnormality consistent with a weak secondary peak at the temperature range specific for MOCV2 (55–57 °C). In addition to the MOCV2 peak, the secondary peak hallmarked MOCV1 in sample 13. Annotated melting curves of the two archival experiments are shown in **Appendix A:** Supplementary Figure **A.2.16**. The total concentrations of template MOCV DNA in these samples were estimated well within the accurately quantifiable levels, 8.72–9.51 × 10^{7} cp/µl in sample 13 and 2.65–2.83 × 10^{7} cp/µl in sample 18 (See **Appendix C** for details). DNA template concentrations of MOCV1 and MOCV2 were estimated at similar orders of magnitude, with MOCV1:MOCV2 ratios at 1.47–1.79 in sample 13 and 2.04–2.96 in sample 18.

4. Discussion

The qPCR-based assay described by Hošnjak et al., (2013) has so far been the most comfortable and sensitive assay for detection, quantification, and genotyping of MOCV. Recently acquired abundant MOCV sequence and genotype information (López-Bueno et al., 2017; Zorec et al., 2018, 2023) revealed the limitations of this and other single mutation or feature detection—related MOCV genotyping assays (Nuñez et al., 1996; Hošnjak et al. 2013), mainly their inability to distinguish between MOCV2 and MOCV3 and misclassification of certain MOCV1 strains as MOCV2. Our newly developed oligo panel resolves these issues by robustly targeting different and disjoint regions of the MOCV genome specific to either MOCV1, MOCV2, or MOCV3.

The highly sensitive amplicon sequencing assay described by Trama et al. (2007) could accurately qualify the currently known MOCV genotypes but, first, lacks PG qualification capabilities and, second, requires a sequencing step for which an additional analytic platform is needed. The new dPCR assay leverages these issues by allowing accurate MOCV genotype determination, quantification, and PG qualification using a single platform and by distinguishing between PGs based on a combination of MOCV genotype and recombination states at *RS1* and *RS2*, as recently suggested (Zorec et al., 2023). This and the fact that the molecular templates targeted by our oligonucleotide panel are distributed across multiple MOCV genomic regions adds another layer of comprehension to the dPCR assay. This can be particularly useful if the assay is used as a triage screen for molecular diversity because it can inherently highlight samples with sequence states that do not entirely match current information. These can then be prioritized for complete genome characterization.

dPCR accuracy and specificity were evaluated using 30 samples including 23 whole DNA isolates from clinical MC samples representing the MOCV genotypes MOCV1 and MOCV2, and the PGs PG1–2 and PG4–5. MOCV3/PG6 was included in the form of three synthetic double-stranded DNA fragments. Nuclease-free water was used in all PCR runs as a non-template negative control and potential carryover control, and commercially available human genomic DNA and two whole DNA isolates of mpox to show absence of cross-reactivity of the oligonucleotides with human DNA and mpox, respectively. Mpox was evaluated because, like several other human-infecting poxviruses, it can cause skin lesions with a similar clinical appearance as MC (Gupta et al., 2023) and because samples were available due to the recent outbreak in 2022 (Resman Rus et al., 2023; Hraib et al., 2022). The results showed perfect specificity and accuracy of dPCR in all categories tested. The MOCV genotype and PG qualifications were consistent with prior information.

Although we had no known samples with PG3, the results demonstrated that the assay can detect all relevant sequence features for accurate and specific detection of this PG (MOCV1, *RS1* E1, *RS2* E1).

We used dPCR to screen 16 MOCV-positive clinical samples that had been previously characterized only partially. Genotyping results were consistent with prior information. Moreover, all samples were either PG1, PG2, PG4, or PG5. Two clinical samples in which dPCR detected both MOCV1 and MOCV2 stood out. Revision of previous results showed that the indication for the presence of both MOCV genotypes already existed during the samples' original handling. This excluded the possibility of sample carryover contamination during the present testing but not prior to their first genotype screens. One of the samples showed conflicting results between methods: it tested as MOCV2 by qPCR but positioned alongside MOCV1 in the sequence phylogeny of the MOCV RNA polymerase gene sequence (*MC079R*). A very exciting interpretation for these double genotype detections is that they are actually simultaneous infections by multiple (two) genotypes. Recombination between MOCV genotypes has been implicated in PG emergence (Zorec et al., 2023). Recombination involves the exchange of sequence segments between two contiguous genome sequences (Brennan et al., 2023), but both need to be present in the same cellular environment. The double genotype detections described here may suggest such infection configurations, but further testing and studies are needed to confirm our findings. Furthermore, in comparison to the melting curve analysis, which was used for genotyping in the qPCR (Hošnjak et al., 2013), testing multiple different disjoint molecular targets in dPCR proved beneficial in the case of the double genotype detections: the result interpretation was much more straightforward.

This study showed that the novel dPCR-based assay is an MOCV detection tool that is as sensitive as the most sensitive assays previously available. Hošnjak et al. (2013) and Trama et al. (2007) reported limits of detection of their assays at 3.3 and 10 cp/µl, respectively. Similarly, dPCR detected and accurately quantified MOCV DNA concentration at 10 cp/µl. Because dPCR is susceptible to positive fluorescence signal saturation, which can result in underestimation of template DNA concentration (Falzone et al., 2020), we suggest either using multiple serial dilutions or using a qPCR pre-screen when viral copy quantification is required, as samples should be diluted to concentration levels within dPCR's operation range: 10–10^5 cp/µl. Here we implemented a qPCR screen to help us choose optimal sample dilutions for accurate quantification based on Cq values. Like the dPCR counterpart, the qPCR screen was also implemented as multiplex PCR using the MOCV genotyping oligo set. Although our assay was implemented in dPCR, equivalent oligo sets can be extended to qPCR to improve assay accessibility. We are aware that dPCR analyses and the specific instrument used in our work may be more costly than standard qPCR systems. However, we believe that the work reported here shows important advantages that dPCR offers flexibility and adaptability of the novel assay.

5. Conclusions

Despite being an important human pathogen and valuable model of poxviral evolution, MOCV remains neglected, and little is known about its evolutionary history and circulating genomic variants, especially in non-privileged countries. With the recent accumulation of novel sequence data, the design weaknesses of available MOCV detection/genotyping assays surfaced, indicating that existing MOCV assays fail at accurate genotyping and capturing sub-genotype level diversity. Because characterization of the complete MOCV genome is an expensive and labor-intensive task, it makes sense to prioritize samples for whole-genome sequencing by diversity triage screening. To meet this demand, we developed a novel assay for comprehensive detection, genotyping, and absolute quantification of MOCV and qualification of PGs through determination of recombination states at *RS1* and *RS2*. The assay was implemented as dPCR and offered sensitive, specific, and accurate detection, genotyping, and PG qualification of MOCV DNA from clinical samples. The novel assay was technically implemented as two multiplex and one singleplex dPCR, one for detection and genotyping, and two for recombination state determinations, which can be performed independently of each other. The novel assay overcomes the limitations of all previously developed MOCV tests with an accurate distinction between MOCV1 and MOCV2, expansion to MOCV3, and comprehensive PG qualification. Furthermore, the dPCR could simultaneously detect and qualify multiple molecular species of MOCV in individual clinical samples. The novel dPCR assay is suitable for MOCV diversity screening and prioritization for characterization at higher levels of comprehension, such as complete genome characterization.

CRediT authorship contribution statement

Tomaž Mark Zorec: Writing – review & editing, Writing – original draft, Visualization, Validation, Software, Methodology, Investigation, Formal analysis, Data curation, Conceptualization. **Lucijan Skubic:** Writing – review & editing, Writing – original draft, Visualization, Validation, Methodology, Investigation, Formal analysis, Data curation, Conceptualization. **Mario Poljak:** Writing – review & editing, Supervision, Resources, Project administration, Funding acquisition, Conceptualization.

Declaration of Competing Interest

The authors declare that they have no known competing financial interests or personal relationships that could have appeared to influence the work reported in this paper.

Acknowledgments

This work was supported by funding received from the EU4H project Expand (grant 101079884), and the Slovenian Research and Innovation Agency (grants P3–0083 and J3–3062). The funders had no role in the design of the study, collection, analyses, or interpretation of data; writing the manuscript; or the decision to publish the results. The authors thank Katarina Resman Rus, PhD, for kindly providing mpox samples for negative controls.

Appendix A. Supporting information

Supplementary data associated with this article can be found in the online version at doi:10.1016/j.jviromet.2024.114993.

References

Agromayor, M., Ortiz, P., Lopez-Estebaranz, J.L., Gonzalez-Nicolas, J., Esteban, M., Martin-Gallardo, A., 2002. Molecular epidemiology of molluscum contagiosum virus and analysis of the host-serum antibody response in Spanish HIV-negative patients. J. Med. Virol. 66, 151–158. https://doi.org/10.1002/jmv.2124.

Blake, N.W., Porter, C.D., Archard, L.C., 1991. Characterization of a molluscum contagiosum virus homolog of the vaccinia virus p37K major envelope antigen. J. Virol. 65, 3583–3589. https://doi.org/10.1128/JVI.65.7.3583-3589.1991.

Brennan, G., Stoian, A.M.M., Yu, H., Rahman, M.J., Banerjee, S., Stroup, J.N., Park, C., Tazi, L., Rothenburg, S., 2023. Molecular mechanisms of poxvirus evolution. mBio 14, e0152622. https://doi.org/10.1128/mbio.01526-22.

Chen, X., Anstey, A.V., Bugert, J.J., 2013. Molluscum contagiosum virus infection. Lancet Infect. Dis. 13, 877–888. https://doi.org/10.1016/S1473-3099(13)70109-9.

Ehmann, R., Brandes, K., Antwerpen, M., Walter, M., Schlippenbach, K.V., Stegmaier, E., Essbauer, S., Bugert, J., Teifke, J.P., Meyer, H., 2021. Molecular and genomic characterization of a novel equine molluscum contagiosum-like virus. J. Gen. Virol. 102, 001357 https://doi.org/10.1099/jgv.0.001357.

Falzone, L., Musso, N., Gattuso, G., Bongiorno, D., Palermo, C.I., Scalia, G., Libra, M., Stefani, S., 2020. Sensitivity assessment of droplet digital PCR for SARS-CoV-2 detection. Int. J. Mol. Med. 46, 957–964. https://doi.org/10.3892/ijmm.2020.4673.

Gupta, A.K., Talukder, M., Rosen, T., Piguet, V., 2023. Differential diagnosis, prevention, and treatment of mpox (monkeypox): A review for dermatologists. Am. J. Clin. Dermatol. 24, 541–556. https://doi.org/10.1007/s40257-023-00778-4.

Hay, R.J., Johns, N.E., Williams, H.C., Bolliger, I.W., Dellavalle, R.P., Margolis, D.J., Marks, R., Naldi, L., Weinstock, M.A., Wulf, S.K., Michaud, C., Murray, C.J.L., Naghavi, M., 2014. The global burden of skin disease in 2010: an analysis of the

prevalence and impact of skin conditions. J. Invest. Dermatol. 134, 1527–1534. https://doi.org/10.1038/jid.2013.446.
Hošnjak, L., Kocjan, B.J., Kušar, B., Seme, K., Poljak, M., 2013. Rapid detection and typing of Molluscum contagiosum virus by FRET-based real-time PCR. J. Virol. Methods 187, 431–434. https://doi.org/10.1016/j.jviromet.2012.11.008.
Hraib, M., Jouni, S., Albitar, M.M., Alaidi, S., Alshehabi, Z., 2022. The outbreak of monkeypox 2022: An overview. Ann. Med. Surg. 79, 104069 https://doi.org/10.1016/j.amsu.2022.104069.
Katoh, K., Standley, D.M., 2013. MAFFT multiple sequence alignment software version 7: improvements in performance and usability. Mol. Biol. Evol. 30, 772–780. https://doi.org/10.1093/molbev/mst010.
Konya, J., Thompson, C.H., 1999. Molluscum contagiosum virus: antibody responses in persons with clinical lesions and seroepidemiology in a representative Australian population. J. Infect. Dis. 179, 701–704. https://doi.org/10.1086/314620.
Koressaar, T., Remm, M., 2007. Enhancements and modifications of primer design program Primer3. Bioinformatics 23, 1289–1291. https://doi.org/10.1093/bioinformatics/btm091.
López-Bueno, A., Parras-Moltó, M., López-Barrantes, O., Belda, S., Alejo, A., 2017. Recombination events and variability among full-length genomes of co-circulating molluscum contagiosum virus subtypes 1 and 2. J. Gen. Virol. 98, 1073–1079. https://doi.org/10.1099/jgv.0.000759.
Nakamura, J., Muraki, Y., Yamada, M., Hatano, Y., Nii, S., 1995. Analysis of molluscum contagiosum virus genomes isolated in Japan. J. Med. Virol. 46, 339–348. https://doi.org/10.1002/jmv.1890460409.
NCBI, 2023. GenBank. ⟨https://www.ncbi.nlm.nih.gov/genbank/⟩ (accessed 10 November 2023).
NCBI, 2023. Nucleotide BLAST. ⟨https://blast.ncbi.nlm.nih.gov/Blast.cgi⟩ (accessed 22 November 2023).
Nuñez, A., Funes, J.M., Agromayor, M., Moratilla, M., Varas, A.J., Lopez-Estebaranz, J.L., Esteban, M., Martin-Gallardo, A., 1996. Detection and typing of molluscum contagiosum virus in skin lesions by using a simple lysis method and polymerase chain reaction. J. Med. Virol. 50, 342–349. https://doi.org/10.1002/(SICI)1096-9071(199612)50:4<342::AID-JMV10>3.0.CO;2-K.
Porter, C.D., Archard, L.C., 1992. Characterisation by restriction mapping of three subtypes of molluscum contagiosum virus. J. Med. Virol. 38, 1–6. https://doi.org/10.1002/jmv.1890380102.
PREMIER Biosoft, 2023. Net Primer. ⟨http://www.premierbiosoft.com/netprimer/⟩ (accessed 22 November 2023).
Resman Rus, K., Zakotnik, S., Sagadin, M., Knap, N., Suljič, A., Zorec, T.M., Mastnak, M., Petrovec, M., Poljak, M., Korva, M., Avšič-Županc, T., 2023. Molecular epidemiology of the 2022 monkeypox virus outbreak in Slovenia. Acta Derm. Alp. Pannonica Adriat. 32, 111–117.
Quan, P.L., Sauzade, M., Brouzes, E., 2018. dPCR: A Technology Review. Sens. (Basel) 18, 1271. https://doi.org/10.3390/s18041271.
Saral, Y., Kalkan, A., Ozdarendeli, A., Bulut, Y., Doymaz, M.Z., 2006. Detection of Molluscum contagiosum virus (MCV) subtype I as a single dominant virus subtype in Molluscum lesions from a Turkish population. Arch. Med. Res. 37, 388–391. https://doi.org/10.1016/j.arcmed.2005.05.020.
Senkevich, T.G., Bugert, J.J., Sisler, J.R., Koonin, E.V., Darai, G., Moss, B., 1996. Genome sequence of a human tumorigenic poxvirus: prediction of specific host response-evasion genes. Science 273, 813–816. https://doi.org/10.1126/science.273.5276.813.
Senkevich, T.G., Koonin, E.V., Bugert, J.J., Darai, G., Moss, B., 1997. The genome of molluscum contagiosum virus: analysis and comparison with other poxviruses. Virology 233, 19–42. https://doi.org/10.1006/viro.1997.8607.
Sherwani, S., Farleigh, L., Agarwal, N., Loveless, S., Robertson, N., Hadaschik, E., Schnitzler, P., Bugert, J.J., 2014. Seroprevalence of Molluscum contagiosum virus in German and UK populations. PLoS One 9, e88734. https://doi.org/10.1371/journal.pone.0088734.
Taghinezhad-S, S., Mohseni, A.H., Keyvani, H., Ghobadi, N., 2018. Molecular screening and single nucleotide polymorphism typing of molluscum contagiosum virus (MCV) from genital specimens, between 2012 and 2015. Iran. Biomed. J. 22, 129–133. https://doi.org/10.22034/ibj.22.2.129.
Thompson, C.H., 1997. Identification and typing of molluscum contagiosum virus in clinical specimens by polymerase chain reaction. J. Med. Virol. 53, 205–211. https://doi.org/10.1002/(sici)1096-9071(199711)53:3<205::aid-jmv4>3.0.co;2-c.
Trama, J.P., Adelson, M.E., Mordechai, E., 2007. Identification and genotyping of molluscum contagiosum virus from genital swab samples by real-time PCR and Pyrosequencing. J. Clin. Virol. 40, 325–329. https://doi.org/10.1016/j.jcv.2007.09.007.
Trčko, K., Poljak, M., Križmarić, M., Miljković, J., 2016. Clinical and demographic characteristics of patients with molluscum contagiosum treated at the University Dermatology Clinic Maribor in a 5-year period. Acta Dermatovenerol. Croat. 24, 130–136.
Trčko, K., Hošnjak, L., Kušar, B., Zorec, T.M., Kocjan, B.J., Križmarić, M., Seme, K., Miljković, J., Luzar, B., Poljak, M., 2018. Clinical, histopathological, and virological evaluation of 203 patients with a clinical diagnosis of molluscum contagiosum. Open Forum Infect. Dis. 5, ofy298 https://doi.org/10.1093/ofid/ofy298.
Untergasser, A., Cutcutache, I., Koressaar, T., Ye, J., Faircloth, B.C., Remm, M., Rozen, S. G., 2012. Primer3–new capabilities and interfaces. Nucleic Acids Res 40, e115. https://doi.org/10.1093/nar/gks596.
Yamashita, H., Uemura, T., Kawashima, M., 1996. Molecular epidemiologic analysis of Japanese patients with molluscum contagiosum. Int. J. Dermatol. 35, 99–105. https://doi.org/10.1111/j.1365-4362.1996.tb03270.x.
Zorec, T.M., Kutnjak, D., Hošnjak, L., Kušar, B., Trčko, K., Kocjan, B.J., Li, Y., Križmarić, M., Miljković, J., Ravnikar, M., Poljak, M., 2018. New insights into the evolutionary and genomic landscape of molluscum contagiosum virus (MCV) based on nine MCV1 and six MCV2 complete genome sequences. Viruses 10, 586. https://doi.org/10.3390/v10110586.
Zorec, T.M., Alm, E., Lind Karlberg, M., Advani, R., Hošnjak, L., Poljak, M., 2023. Comprehensive analysis of 66 complete molluscum contagiosum virus (MOCV) genomes: characterization and functional annotation of 47 novel complete MOCV genomes, including the first genome of MOCV genotype 3, and a proposal for harmonized MOCV genotyping indexing. mBio 14, e0222423. https://doi.org/10.1128/mbio.02224-23.